Inside this Issue

The Measure of Confidence

Agilent Technologies

Enhanced Integration of LA and ICP-MS with ESI's LA Plug-in for ICP-MS MassHunter

Ciaran O'Connor

Laser Ablation Product Marketing Manager, Electro Scientific Industries, New Wave Research, Montana, USA

Introduction

The integration of Laser Ablation with Inductively Coupled Plasma Mass Spectrometry (LA-ICP-MS) often amounts to little more than a trigger cable and a length of tubing to transport the ablated material from the LA to the ICP. Lack of software integration between the two instruments can make the user's workflow complex, often requiring repetition of method setup and sample analysis steps. Now with ESI's NWR ActiveView plug-in for Agilent's ICP-MS MassHunter software, the user can control many LA operations from within ICP-MS MassHunter, to eliminate repetition and simplify the analysis workflow.

A Streamlined Workflow

Figure 1 shows a screenshot of the ActiveView LA plug-in within ICP-MS MassHunter. Direct laser and sequence setup is performed using the different tabs to define LA parameters such as laser energy, frequency, crater size etc., trigger control (synchronization of LA and ICP acquisition), mass flow properties (gas flow) and finally, the LA patterns themselves.

The Pattern Control tab (Figure 2) enables full edit of the LA pattern parameters, in a convenient
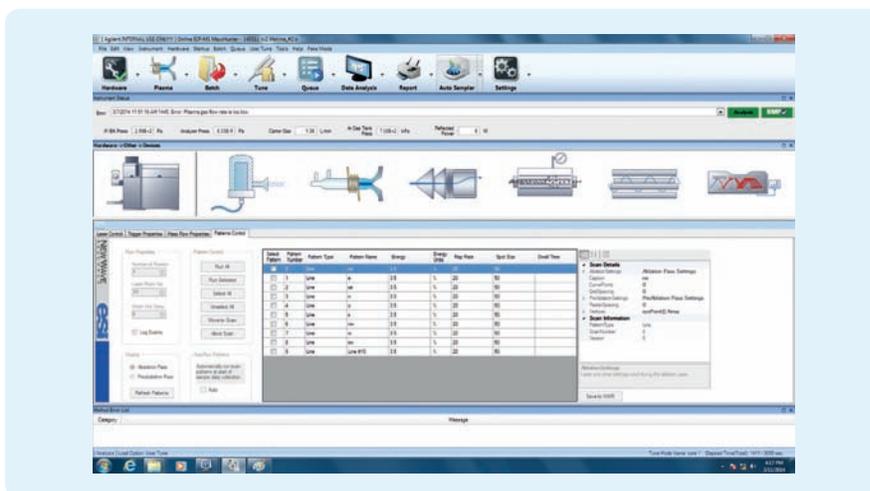
Figure 1. Screenshot of the new ESI NWR ActiveView LA plug-in integrated with ICP-MS MassHunter

spreadsheet format. Changes in pattern parameters are applied automatically to the LA and ICP-MS, avoiding duplication and manual data entry.

The benefit to the user is a more efficient workflow with less repetition and reduced potential for errors. Routine operation is simplified by eliminating the need to regularly switch between two software packages.

Intelligent Triggering and Error Handling

An important benefit of the new plug-in is the ability for the two instruments to share their "ready" status. Failure and error state flags are also exchanged, such as the ICP-MS moving into Standby mode in the event of a utilities failure (loss of exhaust vent flow, or lack of Ar gas, for example). With ActiveView plug-in, the error state is communicated to the LA instrument and the LA sequence is aborted, thus preserving the integrity of the sample for future analysis.

Conclusions

ActiveView plug-in for ICP-MS MassHunter, developed using the Agilent ICP-MS MassHunter software developer's kit, enables more integrated and streamlined operation during automated LA-ICP-MS analysis.

Compatibility and Availability

The new ActiveView plug-in is distributed by ESI and is compatible with ICP-MS MassHunter software version 4.1 and later.

For new customers the installation folder will appear on the desktop of the laser ablation PC and can be installed and configured by the ESI engineer during the install. For existing customers (upgrades) the installation files can be obtained from ESI Technical Support. ActiveView plug-in is customer installable.

Support for the plug-in can be obtained via ESI Technical Support from: **www.esi.com**
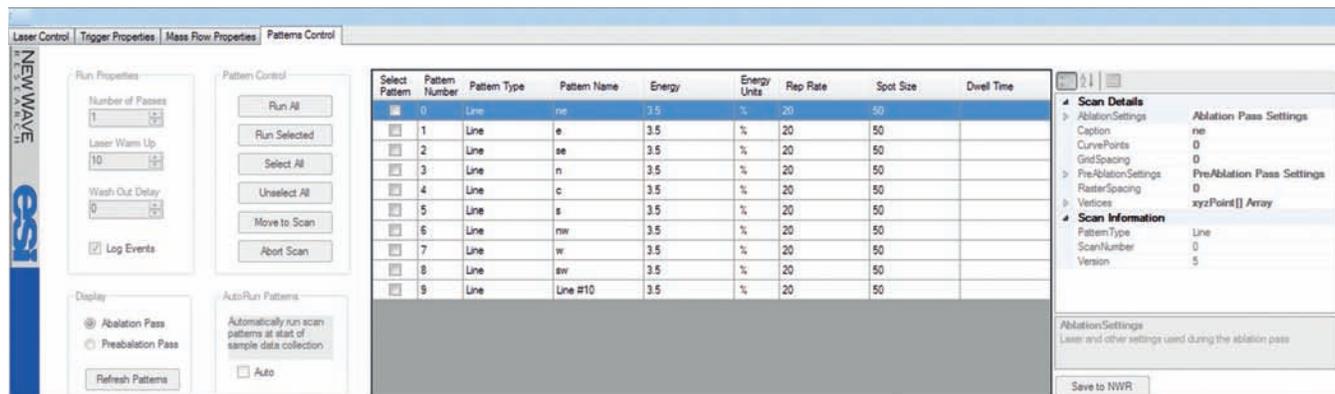
Figure 2. Detailed view of Pattern Control pane of the new ESI NWR ActiveView plug-in for Agilent ICP-MS MassHunter

Determination of the Region of Origin of Chinese Honey by ICP-MS with MPP Chemometric Software

Hui Chen et al

Chinese Academy of Inspection and Quarantine, Beijing China

Introduction

Verifying a food's authenticity is an important aspect of food safety and commerce. Fraudulent mislabeling of foods or adulteration of high value produce with cheaper ingredients is potentially very lucrative, especially if the commercial value of the foodstuff is dependent on its origin, as is often the case with wine, olive oil and honey. Here we describe an ICP-MS method for identifying the botanical and geographical origin of honey, based on the relative concentrations of mineral elements, which are characteristic of the soil composition of the region of production. We used Agilent's Mass Profiler Professional (MPP) software to model the ICP-MS results for 12 elements (Na, Mg, P, K, Ca, Mn, Fe, Cu, Zn, Rb, Sr, and Ba) in 163 reference honey samples, and validated the model using 42 well-characterized reference samples.

Experimental

Samples and Sample Preparation

163 honey samples including varieties produced from linden, vitex, rape, and acacia plants were collected from beekeepers located in 4 geographical locations in China. The honey samples were digested using a MARS 6 microwave oven (CEM Corp., USA). Full details are given in Ref. 1.

Instrumentation

An Agilent 7700x ICP-MS with standard glass concentric nebulizer, quartz double-pass spray chamber, and nickel sampler and skimmer cones was used for the analysis, using the conditions shown in Table 1.

Table 1. ICP-MS operating conditions

RF power (W)	1550
Sample depth (mm)	8
Carrier gas (L/min)	1.1
Plasma gas (L/min)	15
Spray chamber temp (°C)	2
He cell gas (mL/min)	4.3
Number of replicates	3
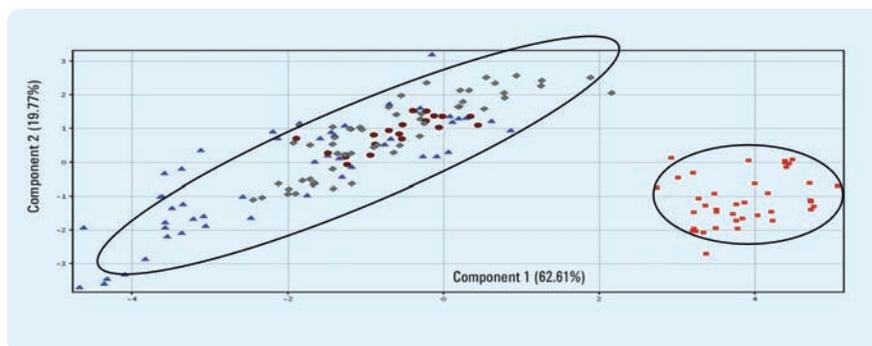
Figure 1. Two first-component scores of honeys from different botanical origins: linden (■), vitex (▲), rape (●), and acacia (◆) honey. All 39 linden honey samples came from Heilongjiang region.

Results and Discussion

ICP-MS analysis of the honey samples showed that the 12 elements of interest varied in concentration depending on the botanical and geographical origin of the honey. However, as there were also variations within the groups of honey samples from the same region, chemometric methods were used for further data processing.

Data Handling using MPP

Agilent's Mass Profiler Professional (MPP) software provides a powerful, integrated chemometrics package for comparing mass spectral data, and displaying complex data in simple, easily interpreted graphical plots. Principal component analysis (PCA), partial least-squares discriminant analysis (PLS-DA) and back-propagation artificial neural network (BP-ANN) were applied to discriminate and classify each honey according to its botanical origin.

PCA is widely used to find the relationships between variables and types of samples. Ten elements, Na, Mg, K, Ca, Mn, Fe, Cu, Rb, Sr, and Ba, displayed statistically significant variation between the honey samples from different botanical origins. The levels of these elements in 163 honey samples were subjected to PCA using the MPP software, and the 10 elements (variables) were reduced to four principal components (PCs). These four PCs explained 93.06% of the total variance.

The loading plot for PC1 and PC2 (Figure 1) shows a clear separation of linden honey from all other samples. To further classify the honey samples using elemental profiling, the data from 121 of the honey samples from different botanical origins was used to build PLS-DA and BP-ANN models in MPP.

The best classification accuracy was achieved using a three-layer BP-ANN model. During the model training process, all 121 honey samples were correctly classified into the four groups representing their botanical origin. A cross-validation procedure utilizing "leave one out" was selected to evaluate the robustness of the developed model. The prediction ability for linden honey was 100% during model cross-validation. The overall accuracy of the prediction ability was slightly lower (92.6%) with accuracies for vitex, rape, and acacia honeys (which included samples collected from 2 or 3 of the geogrpahical regions) of 86.5, 85.7, and 95.1%, respectively.

To further test the stability of the model for prediction, the remaining 42 "unknown" honey samples were classified. The results showed that 41 samples were correctly assigned into the four groups. One acacia honey was wrongly classified as rape honey. The overall prediction accuracy was 97.6%, confirming the robustness of the proposed BP-ANN model for classifying honey.

Conclusions

Elemental profiling by ICP-MS combined with MPP chemometric tools can be used to reliably classify honey samples according to their origin. The excellent accuracy of the BP-ANN prediction model makes it ideally suited for food classification studies, especially in the field of food provenance and adulteration studies, where the elemental content varies depending on the food's origin.

Reference

1. Chemometric Determination of the Botanical Origin for Chinese Honeys on the Basis of Mineral Elements Determined by ICP-MS, Hui Chen, Chunlin Fan, Qiaoying Chang, Guofang Pang, Xueyan Hu, Meiling Lu, and Wenwen Wang, J. Agric. Food Chem. 2014, 62, 2443–2448

Sensitivity Enhancement in LA-ICP-MS by N_2 Addition to Carrier Gas: Application to Radiometric Dating of U-Th-Bearing Minerals

Jean-Louis Paquette, Jean-Luc Piro, Jean-Luc Devidal, Valérie Bosse, Amélie Didier
Laboratoire Magmas & Volcans, Clermont-Ferrand, France

Sébastien Sannac, Yolande Abdelnour
Agilent Technologies, Les Ulis, France

Laser ablation coupled to ICP-MS is widely used in many Earth Sciences applications including dating U-Th-bearing minerals [1]. The impact of adding gases such as H_2, O_2, N_2 or CH_4 to the plasma to enhance the sensitivity has been extensively studied [2, 3, 4]. Conclusions are sometimes divergent, partly due to differences between instruments, tuning configurations and gas mixing systems. A pioneer article on U-Pb dating by LA-ICP-MS [5] described an ICP-MS interface with enhanced pumping capacity, combined with the introduction of a small quantity of N_2 into the carrier gas.

This study aims to optimize the LA-ICP-MS operating conditions for in-situ U-Th-Pb dating in geosciences. Our target was to increase the signal intensity, without degrading the background signal or the oxide ratio. Our strategy was to systematically test N_2 addition alone and in combination with reduced vacuum pressure in the ICP-MS interface.

Instrumentation

The study was carried out using an Agilent 7500 ICP-MS equipped with high sensitivity cs lenses, although similar results have been obtained on an Agilent 7700 ICP-MS and 8800 ICP-QQQ. The standard interface rotary pump was supplemented by the addition of a second rotary pump connected in parallel. The interface pressure of the ICP-MS was monitored by means of a manometer. The pumping rate was adjusted while monitoring the U signal intensity, with the highest signal being obtained at

an expansion chamber pressure of 220 Pa (compared to 320 Pa with the standard single pump configuration). The ICP-MS was coupled to a Resolution M50E excimer 193 nm laser ablation system (Resonetics, Nashua, USA). N_2 flow was regulated by a mass flow controller and added to the He carrier gas downstream from the ablation cell using a T connector. ^{238}U signal intensity tuning was performed using NIST 612 glass reference material (RM), ablated at high energy with a 44 μm-wide single line running at 3 μm/s speed with a repetition rate of 10 Hz and a fluency of 15 J/cm^2. Such aggressive ablation is not suitable for multi-spot U-Pb zircon dating, so analysis of 91500, GEMOC GJ-1 and Mud Tank zircon RMs was also performed using typical analytical conditions of 33 μm, 6 J/cm^2 fluency and repetition rate of 3 Hz in order to minimize inter-element fractionation. LA-ICP-MS operating parameters are given in Table 1.

Table 1. LA-ICP-MS operating parameters

Laser ablation	
Ablation cell & volume	Laurin Technic Ltd® two volumes cell. Volume ca. 1 cm^3
Laser wavelength	193 nm
Pulse width	< 4 ns
Fluency	6 and 15 J/cm^{-2}
Repetition rate	3 and 10 Hz
Spot size	33 and 44 μm
Sampling mode / pattern	Single spot, multi spot or ablation path
Carrier gas	100% He, Ar make-up gas and N_2 combined using the Squid® device.
Cell carrier gas flow (He)	0.70 L/min
ICP-MS	
RF power	1350 W
Make-up gas flow	0.87 L/min Ar
Plasma gas flow	16 L/min
Sampling depth	5 mm
Sensitivity (15 J/cm^2, 44 μm 10 Hz, 3 μm/s line scan speed)	30,000 cps/ppm U
Dead time	35 ns

Results and Discussion

NIST 612 glass reference material
Results are expressed as the enhancement factor of the background corrected signal intensity, normalized to the starting signal intensity acquired in pure argon + helium

carrier gas measured with the standard vacuum pump configuration and no N_2 addition. Only ^{238}U signal enhancement is shown for simplicity, but similar enhancement was observed for ^{232}Th, ^{208}Pb and ^{204}Hg.

With the standard pump configuration, N_2 addition to the carrier gas did not cause a significant increase of ^{238}U signal intensity; at higher N_2 flow rate (>2 mL/min) the U signal slowly decreased (Figure 1). When the second rotary pump was activated (with zero N_2 flow), the ^{238}U signal intensity increased to 1.5 times the level with the standard pump. When N_2 was added, the signal intensity increased rapidly, reaching a maximum enhancement of about 3.5 times for a N_2 flow of 2.5-3 mL/min (Figure 1). The oxide rate, measured as the ^{248}ThO/^{232}Th ratio, remained close to 0.3 % at the optimal N_2 flow. With higher N_2 flow rates, the ^{238}U signal slowly decreased. A significant gain of intensity could be obtained across the whole mass spectrum if the tuning parameters were adjusted.
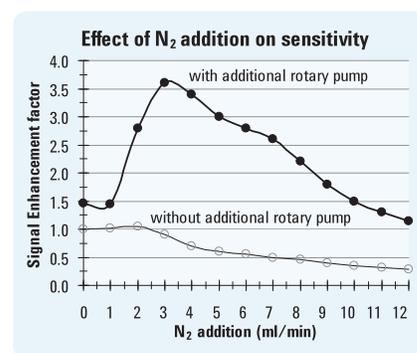
Figure 1. Effect of N_2 addition on sensitivity of ^{238}U.

Zircon reference materials

The 91500 zircon RM is one of the best characterized geochemical RMs for microanalysis [6], so it was selected to standardize the other two samples. 91500 contains moderate U and Pb concentrations, 81 and 15 ppm respectively. GEMOC GJ-1 (grain #61) displays higher U and Pb content, 224 and 20 ppm respectively [1]. Mud Tank zircon megacryst contains lower and more heterogeneous levels [1], with concentrations ranging from 6 to 36 ppm for U and 0.7 to 4.4 ppm for Pb.

We applied the same procedure to the zircon standards as used for the NIST 612 SRM glass RM but using the more typical analytical laser operating conditions previously described (33 μm, 6 J/cm^2, 3 Hz).

Zircon GEMOC GJ-1 Standard
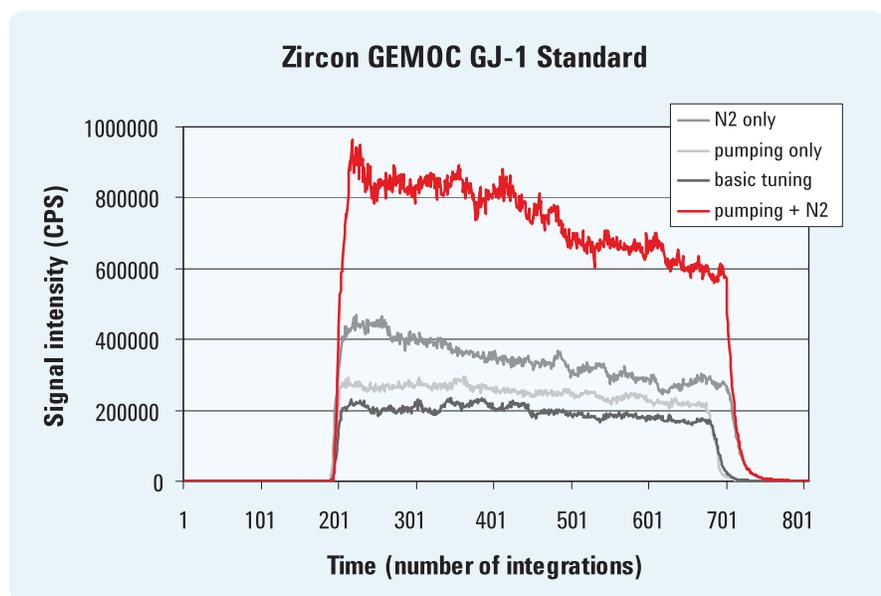
Figure 2. Time resolved profiles of ^{238}U in zircon reference material GEMOC GJ-1.

Figure 2 shows time resolved profiles of ^{238}U during laser ablation of GEMOC GJ-1 zircon standard, with different N$_2$ flow and interface pump configurations. Starting from standard conditions without any gas addition or additional vacuum pump, the signal intensity could be increased by a factor of two by careful adjustment of tuning parameters in the case of additional N$_2$ alone.

Figure 3. Results from twenty consecutive analyses of (a) GEMOC GJ-1 and (b) Mud Tank zircon reference materials showing good agreement with published reference age values.

Additional pump alone provides a gain of 50% signal intensity as reported in Figure 1. Combining N$_2$ and lower interface vacuum pressure, the ^{238}U signal intensity becomes four times higher than under standard conditions. These signal enhancements obtained for the natural zircon samples are broadly similar to those previously obtained on the NIST 612 glass RM.

Twenty consecutive analyses of the GEMOC GJ-1 and Mud Tank zircon RMs provided precise ages of 605.9 ± 3.0 Ma (Figure 3a) and 729.9 ± 4.2 Ma (Figure 3b), respectively. Both results are in good agreement with the published reference age values of 608.5 ± 1.5 Ma [1] and 732 ± 5 Ma [7] respectively.

Conclusions

We have demonstrated that the addition of a low flow of N$_2$ to the carrier gas to increase ion-formation, in combination with lower vacuum pressure to improve ion transmission through the interface, provide an overall gain in the instrument's sensitivity better than 350% at high mass. Enhanced interface pumping alone moderately increases the signal intensity, whereas the addition of N$_2$ alone has minimal effect.

The addition of N$_2$ mostly produces thermal [e.g. 2, 8, 9] and geometric [10] effects on the plasma and consequently improves the vaporization of particles and possibly

ensures better ionization efficiency. The combination of mixed gas plasma and more efficient pumping of the interface vacuum is not a new approach, but it has not previously been studied systematically. The complete understanding of this complex interaction requires further investigation. This increased sensitivity allowed us to date Archean zircons in petrographic thin sections with only a 5-10 μm laser spot size [11] as well as very young and radiogenic Pb-depleted Quaternary zircon crystals [12].

References

1. Jackson S.E., Pearson N.J., Griffin W.L. and Belousova E. (2004), Chemical Geology, 211, 47-69.
2. Hu Z., Gao S., Liu Y., Hu S., Chen H. and Yuan H. (2008), Journal of Analytical Atomic Spectrometry, 23, 1093-1101.
3. Guillong M. and Heinrich C.A. (2007), Journal of Analytical Atomic Spectrometry, 22, 1488-1494.
4. Fliegel D., Frei C., Fontaine G., Hu Z., Gao S. and Günther D. (2011), Analyst, 136, 4925-4934.
5. Hirata T. and Nesbitt R.W. (1995), Geochimica et Cosmochimica Acta, 59, 2491-2500.
6. Wiedenbeck M., Alle P., Corfu F., Griffin W.L., Meier M., Oberli F., von Quadt A., Roddick J.C. and Spiegel W. (1995), Three natural zircon standards for U-Th-Pb, Lu-Hf, trace elements and REE analyses. Geostandard Newsletter, 19, 1-23.
7. Black L.P. and Gulson B.L. (1978), BMR Journal of Australian Geology and Geophysics, 3, 227-232.
8. Choot E.H. and Horlick G. (1986), Spectrochimica Acta Part B: Atomic Spectroscopy, 41, 889-906.
9. Durrant S.F. (1994), Fresenius Journal of Analytical Chemistry, 349, 768-771.
10. Eggins S.M. et al. (2005), Quaternary Science Reviews, 24, 2523-2538.
11. Rizo H., Boyet M., Blichert-Toft J., O'Neil J., Rosing M. and Paquette J.L. (2012), Nature, 491, 96-100.
12. Hurai V., Paquette J.L., Huraiová M. and Sabol M. (2012), Geological Magazine, 149, 989-1000.
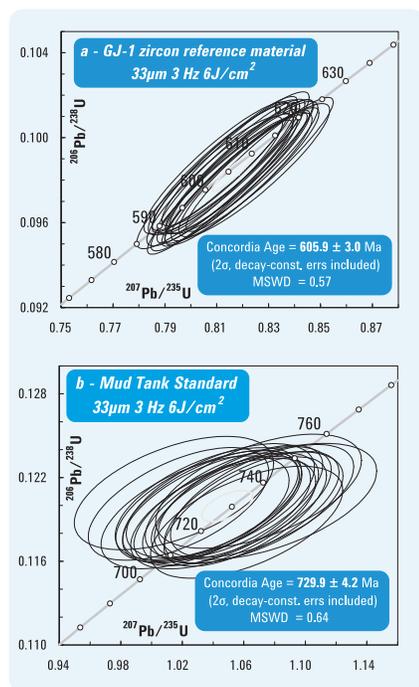
Speciation of Volatile Bromo- and Iodo-Disinfection By-Products by GC-ICP-MS

Armando Durazo and Shane A. Snyder

Department of Chemical & Environmental Engineering, University of Arizona, USA

www.snyderlab.arizona.edu

Figure 1. Log/log plot of a calibration curve for [127]I prepared from 1-bromo-4-iodobenzene (left panel) and an overlay of [127]I peak intensities for calibration standards (ranging from 0.0 to 25 ppb) examined in this work, including a calibration blank (right panel). The retention time for this compound is 20.6 minutes.

Introduction

Water naturally contains differing levels of chloride, bromide, and iodide ions. At normal levels, these ions are not harmful to human health; however, these halides can be incorporated into organic structures when water containing these ions is treated using oxidative processes such as chlorination, ozonation, and chloramination [1, 2]. The oxidative conditions employed in the treatment process can convert these halides into "activated" forms, which can then react with organics present in wastewater to form halogenated disinfection byproducts (DBPs) [3], where many species are unidentified [4].

While the level of some DBPs in drinking water is regulated by the United States EPA, the regulated DBPs are a small list of identifiable compounds [5]. Given that iodinated and brominated DBPs are more toxic than their chlorinated analogs [6-8], it is prudent that occurrence data is acquired quickly in order to better understand the magnitude and prevalence of these emerging DBPs. Most analytical methods such as EPA method 551.1 employ GC with electron capture detection (GC-ECD) for determining the concentrations of volatile halogenated DBPs in extracts prepared from waters. These methods are limited in their ability to differentiate halogenated species from each other, or from other interfering non-halogenated species.

More selective methods do exist for determining halogenated DPBs using GC-MS or GC-MS/MS, but these techniques have limited ability to screen for unidentified halogenated molecules in a single analysis, due to ionization issues. Chemical Ionization (CI) does not ionize all types of organic molecules, and electron impact (EI) can lead to excessive, undesirable in-source fragmentation. In addition, GC-MS/MS analysis (which relies on the collisional loss of halogen atoms from a precursor ion) is limited by the inefficient fragmentation of halogenated precursor ions into monatomic halogen product ions (i.e., Br^+ and Br). In this work, we used GC-ICP-MS to examine and quantitate these halogenated DBPs.

Experimental

Sample Preparation

Municipal wastewater samples were collected from geographically separated areas. Samples were split in two, with one half untreated and the other half treated with aqueous monochloramine. For extraction, 35 mL of these wastewater samples were extracted using 5 mL of MTBE in a modified version of EPA method 551.1. The organic layers were carefully separated and then placed into 2.0 mL amber GC vials (Agilent).

Instrumentation

This study was performed using an Agilent 7890A GC coupled to an Agilent 7700x ICP-MS using an Agilent GC-ICP-MS interface kit (part number G3158C). The instrument conditions used are listed below:

GC:
- Agilent 30 m HP-5 analytical column (320 µm x 0.25 µm)
- 200 °C inlet & 260 °C transfer line/injector temperatures
- Pulsed splitless injection (10 psi until 0.75 min, 5.8 psi afterwards)
- Oven 37 °C for 6 min, then 10 °C/min rise to 260 °C, then hold for 11 min.

ICP-MS:
- No gas mode; time resolved analysis (TRA) for masses 79, 81, and 127
- 0.15 second integration times
- 3.0 mm sampling depth
- 700 W RF power
- 0.4 L/min dilution gas (Ar) delivered to transfer line
- Calibration standards prepared in MTBE using 1-bromo-4-iodobenzene (0, 1, 2, 5, 10, 25, 100 ng/mL).

Analysis of Calibration Standards & Samples

A representative calibration is shown in Figure 1 for 1-bromo-4-iodobenzene, which elutes at 20.6 minutes. Iodine was detected in all non-zero calibration standards (Figure 1) and bromine in all standards with (compound) concentrations above 5 ng/mL.

Wastewater samples were then analyzed before and after treatment with monochloramine. The reaction with monochloramine leads to an increase in the concentration of brominated and iodinated species in the extracts (Figure 2). These data reveal several interesting facts. First, there are volatile halogenated organics present in wastewaters prior to chloramination. Secondly, some of these species remain unchanged following monochloramine treatment, while others are removed (and likely transformed into new halogenated DBPs). This implies that non-halogenated organics in untreated wastewaters may also be converted into new halogenated DBPs in the same way.
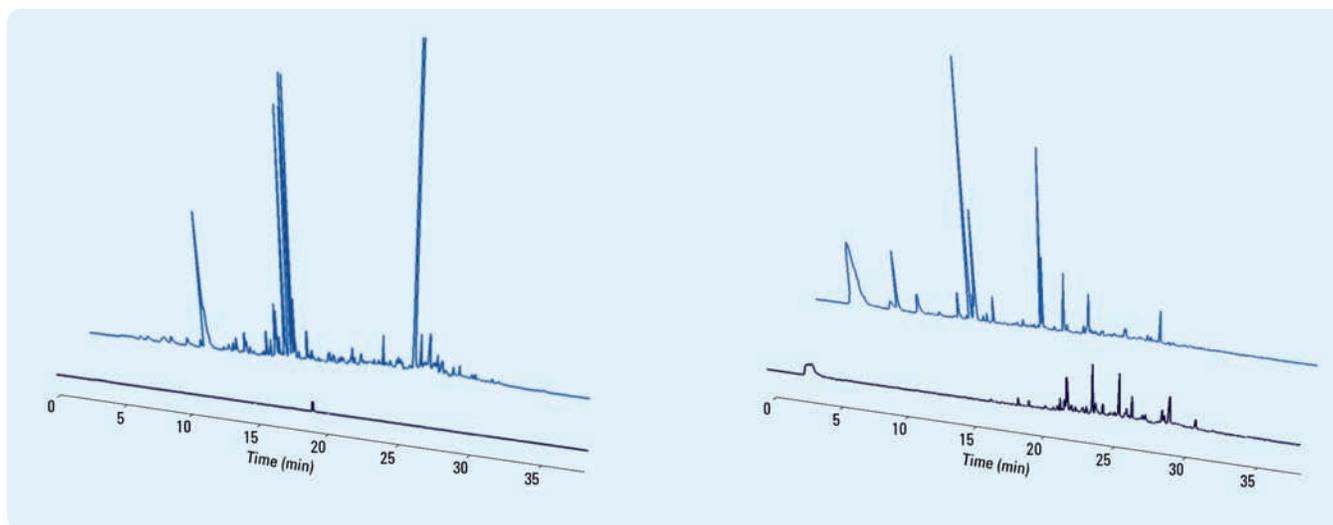
Figure 2. 81Br (Left) and 127I (Right) GC-ICP-MS chromatograms obtained from MTBE extracts prepared from a representative wastewater sample before chloramination (purple line, front) and after chloramination (blue line, behind). Intensity scales are identical for both plots. Chromatograms are not background-subtracted.

Results and Discussion

The results of our study indicate that the chloramination of wastewater samples dramatically changes the concentration and speciation of halogenated volatile organics in these waters. The effects of chloramination are most apparent in the differences between chromatograms for brominated and iodinated DBPs. The total level of volatile organohalogen compounds increases after chloramination (Table 1) and there is an increased presence of more highly volatile iodinated DBPs.

Table 1. Total concentrations of elemental bromine and iodine in water samples before and after chloramination

	Blank extract	Before ClNH$_2$	After ClNH$_2$
Bromine (ppb)	103	1134	98229
Iodine (ppb)	93	490	777

Conclusions

We have demonstrated the use of GC-ICP-MS to determine the presence, transformation, and formation of halogenated DBPs in wastewaters that are treated by chloramination. The method allows for easy tuning, chromatographic separation of an array of diverse compounds, and interference-free, high sensitivity analysis for halogens covalently bound within organic molecules. The use of compound-independent calibrations (CICs) allows us to quantitate the halogen contents of these compounds based on the responses obtained from a commercially available dihaloaromatic.

An additional benefit to using GC-ICP-MS for the analysis of these complex mixtures of halogenated organics is the element-specificity of the technique compared to other halogen detection methodologies like GC-ECD. In the near future, we aim to identify these DBPs using GC-QToF and to investigate water treatment technologies that will minimize the formation of halogenated DBPs.

References

1. Richardson, S.D., et al., Occurrence and Mammalian Cell Toxicity of Iodinated Disinfection Byproducts in Drinking Water. *Environmental Science & Technology*, 2008. **42**(22): p. 8330-8338.
2. Sharma, V.K., R. Zboril, and T.J. McDonald, Formation and toxicity of brominated disinfection byproducts during chlorination and chloramination of water: A review. *Journal of Environmental Science and Health, Part B*, 2013. **49**(3): p. 212-228.
3. Hua, G. and D.A. Reckhow, Effect of pre-ozonation on the formation and speciation of DBPs. *Water Research*, 2013. **47**(13): p. 4322-4330.
4. Jeong, C.H., et al., Occurrence and Toxicity of Disinfection Byproducts in European Drinking Waters in Relation with the HIWATE Epidemiology Study. *Environmental Science & Technology*, 2012. **46**(21): p. 12120-12128.
5. United States EPA, National primary drinking water regulations: Stage 2 disinfectants and disinfection byproducts rule. *Fed. Regist.*, 2006. **71**(2): p. 387– 493.
6. Krasner, S.W., et al., Occurrence of a New Generation of Disinfection Byproducts. *Environmental Science & Technology*, 2006. **40**(23): p. 7175-7185.
7. Smith, E.M., et al., Comparison of Byproduct Formation in Waters Treated with Chlorine and Iodine: Relevance to Point-of-Use Treatment. *Environmental Science & Technology*, 2010. **44**(22): p. 8446-8452.
8. Woo, Y.-T., et al., Use of Mechanism-Based Structure-Activity Relationships Analysis in Carcinogenic Potential Ranking for Drinking Water Disinfection By-Products. *Environmental Health Perspectives Supplements*, 2002. **110**: p. 75.

More Information

See Agilent publication:
An Examination of the Presence, Formation, and Transformation of Volatile Halogenated Organic Species in Wastewater Extracts Using GC-ICP-MS, publication number 5991-4398EN, which is available at **www.agilent.com/chem**

Agilent Continues to Drive Innovation in Atomic Spectroscopy with 5100 ICP-OES

Agilent 5100 Synchronous Vertical Dual View ICP-OES

2014 has been a landmark year for significant developments within Agilent's atomic spectroscopy product range. Following the introduction of the 7900 ICP-MS and 4200 MP-AES platforms in January, Agilent has further reinforced its position as a technology leader in atomic spectroscopy with the introduction of the Agilent 5100 ICP-OES.

The new system features innovative technology that enables it to detect both radial and axial view measurements of a robust vertically-orientated plasma in a single reading. This is in contrast to conventional dual view systems that require multiple measurements per sample for all wavelengths. The 5100 achieves synchronous vertical dual-view (SVDV) measurements thanks to innovative Dichroic Spectral Combiner (DSC) technology. The benefits to customers include faster sample run times, less argon gas consumption and a capability to measure the most challenging samples, from high matrix to volatile organic solvents.

New ICP Expert software that includes a series of pre-set method templates and hardware developments such as plug-and-play torch ensure reliable and reproducible instrument set-up and simplified method development by all users, irrespective of their level of expertise.

The 5100 ICP-OES is suited to labs doing food, environmental and pharmaceuticals testing, as well as mining and industrial applications.

Learn More at:
www.agilent.com/chem/5100icpoes

This information is subject to change without notice.

© Agilent Technologies, Inc. 2014
Printed in the U.S.A. July 31, 2014
5991-4967EN

Which Atomic Spectroscopy Technique is Best Suited to Your Analytical Needs?

Agilent provides the most comprehensive and innovative range of instruments for inorganic analysis of liquid samples including: Flame AAS; Fast Sequential Flame AAS; Graphite Furnace AAS (GFAAS); Vapor Generation AAS; MP-AES; synchronous vertical dual-view ICP-OES, ICP-QMS and ICP-QQQ. Selecting the best technique for any given application will depend on a number of factors such as the required detection limits, number of elements per sample, sample throughput, target analytes, linear dynamic range, TDS, regulatory compliance, lab safety, available budget and experience of lab personnel. The two main considerations (number of samples & analytes and detection limit capability) are shown in Figure 1.
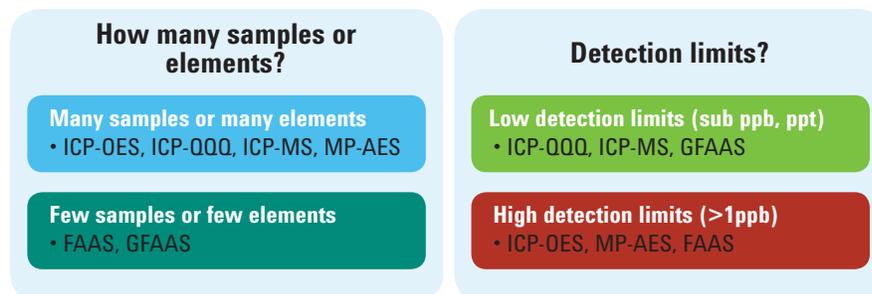

Figure 1. Number of sample or analytes vs detection limit capability

Learn more about Agilent's portfolio of AA, MP-AES, ICP-OES, ICP-MS, ICP-QQQ instrumentation by downloading:
• **Brochure:** Leading the Way in Atomic Spectroscopy Technology, 5990-6443EN.

Conferences. Meetings. Seminars.

• **Thailand, Malaysia and Singapore:** Spectroscopy users are welcome to join our *Annual Atomic Spectroscopy User Meetings* and learn about new developments from Agilent and share experiences. The dates are: **Monday**, August 18, Bangkok, **Wednesday**, August 20, Kuala Lumpur **Friday**, August 22, Singapore
Register online at **agilent.com/chem/atomic_user_meeting**
• **JASIS,** September 3-5, 2014, Makuhari Messe, Japan, **jasis.jp/2014/en**
• **Society of Minerals Analysis,** September 16-18, 2014, Elko, NV, USA, **sma-online.org**
• **ICP-MS User Meeting,** September 15-18, 2014 Helmholtz-Zentrum, Geesthacht, Germany, **hzg.de/mw/icpms_anwendertreffen2014**
• **CMA Saskatoon**, September 21-25, 2014, Saskatchewan, Canada, **cma2014saskatoon.ca**
• **SciX**, September 28-October 3, 2014, Reno, NV, USA, **scixconference.org**
• **SupplySide West**, October 6-10, 2014, Las Vegas, NV, USA, **west.supplysideshow.com**
• **European Winter Conference on Plasma Spectrochemistry**, February 22-26, 2015, Münster, Germany, **ewcps2015.org**

Agilent ICP-MS Publications

To view and download the latest ICP-MS literature, go to **www.agilent.com/chem/icpms** and look under **"Literature Library"**

• **Application note:** Agilent 7900 ICP-MS simplifies drinking water analysis, 5991-4938EN
• **Brochure:** Atomic Spectroscopy Portfolio Brochure, 5990-6443EN

Agilent ICP-MS Journal Editor

Karen Morton for Agilent Technologies
e-mail: icpms@agilent.com

Agilent Technologies